

## Anisotropic classical chain: Numerical calculations of thermodynamic properties

F. Boersma, W. J. M. de Jonge, and K. Kopinga

*Department of Physics, Eindhoven University of Technology, 5600 MB Eindhoven, The Netherlands*

(Received 7 July 1980)

Thermodynamic properties are computed for the classical linear chain with orthorhombic anisotropy in an external magnetic field. Special attention has been given to crossover effects between different model systems as a function of temperature and field. The ordering temperature of quasi-one-dimensional systems is computed as a function of the interchain interactions and the anisotropy. Results are compared with other theories.

### I. INTRODUCTION

The problem of an accurate theoretical description of the behavior and the properties of an infinite array of interacting particles (or spins) has attracted considerable attention during the last decade. Many simplified models have been introduced, among them the classical model<sup>1</sup> in which the interacting spins are treated as classical vectors. It appeared that, within this approximation, analytic expressions for the thermodynamical variables of an infinite chain can be obtained, provided the interaction is isotropic (Heisenberg exchange). Moreover, it has been shown by various experiments<sup>2</sup> that for several thermodynamic properties classical behavior, which in fact corresponds to the limit of infinite spin quantum number  $S$ , can be found already in real systems with  $S \geq \frac{5}{2}$  (or sometimes even lower).

In view of this, the model has been extensively used in the interpretation of experimental results specifically for  $Mn^{++}$  ( $S = \frac{5}{2}$ ) compounds. Extensions to the isotropic theory were given by Blume *et al.*<sup>3</sup> and Lovesey *et al.*,<sup>4</sup> who reported numerical solutions for the classical chain in an applied field and by Loveluck *et al.*,<sup>5</sup> who introduced *uniaxial* anisotropy in the system. All these approximations have in common that the system still contains rotational symmetry around some axis. Experimental evidence, however, indicated that even a small orthorhombic anisotropy can have a rather drastic effect on some thermodynamic variables.<sup>6</sup> This effect originates from the fact that at lower temperatures ultimately this anisotropy invokes an Ising-like behavior, which means an *exponential* increase of the correlation length when  $T$  approaches zero. As the other thermodynamic variables are all somehow related to the correlation function, it stands to reason that introduction of a general anisotropy can strongly modify their behavior. Therefore it seemed worthwhile to perform calculations on the classical chain with orthorhombic anisotropy. Preliminary results have been reported, mainly in relation to the

explanation of the anomalous field dependence of  $T_N$  in quasi-one-dimensional (1D) Heisenberg systems.<sup>7</sup>

The organization of this paper is as follows. We will continue with a section containing the relevant theoretical background, followed by Sec. III which describes the numerical details of the calculations. The final section contains selected results and some general conclusions.

### II. THEORY

Before we go into the details of the theoretical treatment of the problem, we would first like to discuss some more general aspects related to the starting point: that is the Hamiltonian. Since a large number of papers appeared on magnetic model systems, also a large number of different Hamiltonians have been introduced. Judging from the inconsistent use of various names for these model systems, apparently some confusion does exist about the nomenclature of the limiting cases.<sup>2,8,9</sup> Since we will refer to several of these model Hamiltonians, we would like to start with a review of the classification of relevant Hamiltonians, which we will be using in this paper.

Let us consider a Hamiltonian of the following general form

$$\mathcal{H} = -2 \sum_{i < j} (J^{xx} S_i^x S_j^x + J^{yy} S_i^y S_j^y + J^{zz} S_i^z S_j^z) - D \sum_i (S_i^z)^2 \quad (1)$$

Let us first discuss the case  $D = 0$ . In that case, whatever the further restrictions on  $J^{\alpha\alpha}$ , we are dealing with a three component ( $n = 3$ ) spin system and hence

$$(S_i^x)^2 + (S_i^y)^2 + (S_i^z)^2 = S(S+1)$$

In Table I we have tabulated the model systems and their nomenclature, resulting from restrictions and simplifications of the interaction  $J^{\alpha\alpha}$ . In order to reduce the degrees of freedom of the interacting

TABLE I. Nomenclature of the different model systems, characterized by the Hamiltonian

$$\mathfrak{H} = -2 \sum_{i < j} (J^{xx} S_i^x S_j^x + J^{yy} S_i^y S_j^y + J^{zz} S_i^z S_j^z) - D \sum_i (S_i^z)^2 .$$

References are confined to one-dimensional systems.

	Interaction	Nomenclature	References		
			$S = \infty$	$S = \frac{1}{2}$	$S > \frac{1}{2}$
$D = 0$ spin dimensionality $n = 3$	isotropic $J^{xx} = J^{yy} = J^{zz}$	Heisenberg	1,10	11	12
	in a plane $J^{xx} = J^{yy}, J^{zz} = 0$	$XY$		13	
	along one axis $J^{xx} = J^{yy} = 0, J^{zz}$	$Z$	14		15
$D \rightarrow -\infty$ spin dimensionality $n = 2$	isotropic $J^{xx} = J^{yy}$	planar	10,16,17		
	along one axis $J^{xx}, J^{yy} = 0$	planar Ising			
$D \rightarrow +\infty$ spin dimensionality $n = 1$	$J^{zz}$	Ising	10	18	

spins, one might state that  $n = 2$  or  $1$  and equivalently insert

$$(S_i^x)^2 + (S_i^y)^2 = S(S + 1)$$

or

$$(S_i^z)^2 = S(S + 1) .$$

In physical reality, however, these models may be thought to originate as limiting cases from the Hamiltonian Eq. (1) including  $D$ . This limit may be obtained either theoretically by  $D$  approaching  $+$  or  $-$  infinity or physically (as we will discuss later on) by  $T$  approaching zero for finite values of  $D$ .

For negative values of  $D$ , there is, so to speak, a penalty for the spins to be directed along the  $z$  direction. In the limit of  $D \rightarrow -\infty$  a  $z$  component of the spins is ultimately forbidden. Hence the spin has been transformed into a two-dimensional vector.<sup>17</sup> An illustration of this behavior is shown in Fig. 1. In this figure the probability density to find a spin at an angle  $\theta$  from the  $z$  direction is shown for different values of  $D$ . In this example the results were computed with the 1D classical model. For  $D \rightarrow -\infty$  the

curve narrows down to a  $\delta$  peak at  $\theta = \frac{1}{2}\pi$ , illustrating the reduction of the degrees of freedom of the spin to the  $XY$  plane ( $n = 2$ ). For positive values of  $D$  we get an analogous picture. The probability density is now peaking at  $\theta = 0$  and  $\pi$ , which means that in the limit of  $D \rightarrow \infty$  the system has only spin components along the  $z$  direction ( $n = 1$ ). This last model is commonly referred to as the Ising model and should be distinguished in principle from the ( $n = 3$ )  $Z$  model. The same distinction should be made between the ( $n = 3$ )  $XY$  model and the ( $n = 2$ ) planar model also tabulated in Table I. Inspection of this table reveals further that such a distinction leads to the so-called planar Ising model which, to our knowledge, so far escaped the attention of theoreticians, since no results have been reported. We will return to the behavior of these model systems in the discussion in the last section.

Now, we consider the solution of the classical model for a one-dimensional system containing orthorhombic anisotropy. Unless stated otherwise, the spins will be considered as three-dimensional unit vectors ( $n = 3$ ) and anisotropic terms in the Hamil-

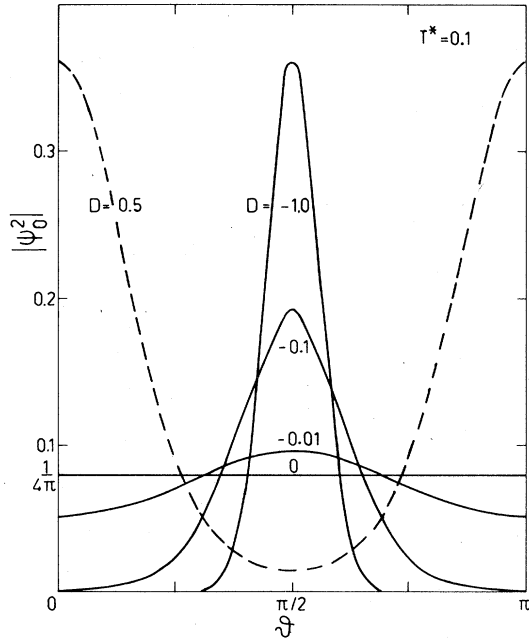


FIG. 1. Probability density as function of the azimuthal angle  $\theta$  for different values of the anisotropy parameter  $D$  [ $T^* = kT/2|J|S(S+1) = 0.1$ ].

tonian will be relatively small. If only nearest-neighbor interactions are present, the Hamiltonian describing the properties of a chain can be written as

$$\mathcal{H}_{\text{chain}} = \sum_{i=-\infty}^{+\infty} \mathcal{H}(\vec{S}_i, \vec{S}_{i+1}) . \quad (2)$$

We will consider three contributions to  $\mathcal{H}$ , a term due to the exchange interaction  $\mathcal{H}_{\text{ex}}$ , a term due to an external magnetic field  $\mathcal{H}_F$ , and a term due to a so-called single-ion anisotropy  $\mathcal{H}_{\text{si}}$ . The orthorhombic exchange part of the Hamiltonian,  $\mathcal{H}_{\text{ex}}$ , is written as

$$\mathcal{H}_{\text{ex}} = -2\tilde{S}^2 \sum_{\alpha} J^{\alpha\alpha} s_i^{\alpha} s_{i+1}^{\alpha} , \quad \alpha = x, y, z . \quad (3)$$

The other terms are given by

$$\mathcal{H}_F = -g\mu_B \frac{1}{2} H \tilde{S} (s_i^z + s_{i+1}^z) \quad (4)$$

and

$$\mathcal{H}_{\text{si}} = -\frac{1}{2} \tilde{S}^2 \sum_{k=i, i+1} \{ D [(s_k^z)^2 - \frac{1}{3}] + E [(s_k^x)^2 - (s_k^y)^2] \} . \quad (5)$$

In these expressions  $\vec{S}_i$  is a classical unit vector located at site  $i$ . The actual spins are normalized by taking<sup>1</sup>

$$\tilde{S} = \sqrt{S(S+1)} . \quad (6)$$

In the presentation of our calculations and the discussion of the results, the effect of anisotropy in  $\mathcal{H}_{\text{ex}}$  will be emphasized. We like to note, however, that anisotropy in  $\mathcal{H}_{\text{si}}$  gives rise to essentially similar effects. The Hamiltonian  $\mathcal{H}_{\text{ex}}$  can be written in a more convenient form by defining the anisotropy parameters  $e_z$  and  $e_{xy}$  as

$$e_z = \frac{|J_{zz}| - |J|}{|J|} , \quad e_{xy} = \frac{|J_{xx}| - |J_{yy}|}{|J|} , \quad (7)$$

where the interaction  $J$  is given by

$$J = \frac{1}{3} (J_{xx} + J_{yy} + J_{zz}) . \quad (8)$$

A positive value of  $J$  indicates a ferromagnetic coupling. Substitution of Eqs. (7) and (8) into Eq. (3) yields

$$\begin{aligned} \mathcal{H}_{\text{ex}} = & -2J\tilde{S}^2 [\vec{S}_i \cdot \vec{S}_{i+1} \\ & + e_z (s_i^z s_{i+1}^z - \frac{1}{2} s_i^x s_{i+1}^x - \frac{1}{2} s_i^y s_{i+1}^y) \\ & + \frac{1}{2} e_{xy} (s_i^x s_{i+1}^x - s_i^y s_{i+1}^y)] . \quad (9) \end{aligned}$$

To handle this classical Hamiltonian we will use the transfer-matrix formalism,<sup>19</sup> which will be shortly reviewed below. The classical spin vector components are denoted in spherical representation

$$\begin{aligned} \vec{S}_i = & (s_i^x, s_i^y, s_i^z) \\ = & (\cos\phi_i \sin\theta_i, \sin\phi_i \sin\theta_i, \cos\theta_i) . \quad (10) \end{aligned}$$

Assuming periodic boundary conditions,  $\vec{S}_{N+1} = \vec{S}_1$ , the partition function of the chain can be written as

$$Z_N = \int_1 \cdots \int_N d\vec{S}_1 d\vec{S}_2 \cdots d\vec{S}_N \prod_{i=1}^N K(\vec{S}_i, \vec{S}_{i+1}) , \quad (11)$$

where the kernel  $K$  is given by

$$\begin{aligned} K(\vec{S}_i, \vec{S}_{i+1}) = & \exp[-\beta \mathcal{H}(\vec{S}_i, \vec{S}_{i+1})] , \quad (12) \\ \beta = & 1/kT , \end{aligned}$$

and  $d\vec{S}_i$  is a solid angle segment. As the expectation value of an arbitrary thermodynamic variable  $A$  can be expressed as

$$\langle A \rangle = \frac{\text{Tr}(AK)}{\text{Tr}(K)} , \quad (13)$$

it is convenient to evaluate the traces appearing in Eq. (13) in terms of the eigenvalues and eigenfunctions of the kernel given in Eq. (12), which are defined by the homogeneous integral equation

$$\begin{aligned} \int d\phi_{i+1} \int d\theta_{i+1} \sin\theta_{i+1} \\ \times K(\vec{S}_i, \vec{S}_{i+1}) \psi(\vec{S}_{i+1}) = \lambda \psi(\vec{S}_i) . \quad (14) \end{aligned}$$

Because of the linearity of this equation, there exists

a complete orthonormal set of solutions. Furthermore, all eigenvalues will be real, due to the symmetry of the kernel.<sup>20</sup>

Since by means of the transfer-matrix formalism all thermodynamic variables can be expressed in the eigenvalues and eigenfunctions of an integral equation, the remaining task is to solve the eigenvalue problem given in Eq. (14). In previous papers on the subject,<sup>3-5</sup> problems were considered which contained rotational symmetry around the  $z$  direction, and hence it was possible to separate the  $\phi$  dependence. In this way the integrals over  $\phi_{i+1}$  could be performed explicitly. In the problem discussed in this paper, however, this uniaxial symmetry is not present. As it is very inconvenient to handle a problem with two integration variables numerically, we will eliminate the  $\phi$  integration. To this end we introduce the following Fourier expansions

$$\psi_n(\theta_i, \phi_i) = \frac{1}{(2\pi \sin\theta_i)^{1/2}} \sum_{m'=-\infty}^{+\infty} \phi_{m'n}(\theta_i) e^{im'\phi_i} \quad (15)$$

and

$$K(\bar{s}_i, \bar{s}_{i+1}) = \frac{1}{2\pi} \sum_{m=-\infty}^{+\infty} \sum_{l=-\infty}^{+\infty} K_{ml}(\theta_i, \theta_{i+1}) \times \exp[i(m\phi_i - l\phi_{i+1})] \quad (16)$$

The indices  $i, i+1$  will be replaced by 1, 2, which is allowed by the translational invariance of the problem. Substitution of Eqs. (15) and (16) into Eq. (14) leads, because of the orthogonality of the functions  $\exp(-im\phi)$ , to the set of coupled integral equations

$$\sum_{l=-\infty}^{+\infty} \int_0^\pi d\theta_2 (\sin\theta_1 \sin\theta_2)^{1/2} K_{ml}(\theta_1, \theta_2) \Phi_n(\theta_2) = \lambda_n \Phi_{mn}(\theta_1), \quad (17)$$

$$m = 0, \pm 1, \pm 2, \dots,$$

in which the  $K_{ml}$  are given by the inverse Fourier transform of Eq. (16), i.e.,

$$K_{ml}(\theta_1, \theta_2) = \frac{1}{2\pi} \int_{-\pi}^\pi d\phi_2 \int_{-\pi}^\pi d\phi_1 K(\bar{s}_1, \bar{s}_2) \times \exp(-im\phi_1 + il\phi_2) \quad (18)$$

The indices  $n$  will be omitted for convenience.

It is obvious that Eq. (17), the central problem in this section, cannot be solved without further simplifications. Before tackling the problem with numerical methods, we will show that this set of equations can be separated into four smaller subsets, using the  $C_{2v}$

point symmetry of the Hamiltonian Eq. (2). From the fact that the kernel  $K$  must be invariant under the symmetry operations belonging to the point group  $C_{2v}$ , it follows that

$$K_{ml}(\theta_1, \theta_2) = 0 \quad \text{for } |m-l| = \text{odd} \quad (19)$$

and

$$K_{ml}(\theta_1, \theta_2) = K_{-m-l}(\theta_1, \theta_2) \quad (20)$$

These equations can also be derived algebraically from the properties of the modified Bessel functions, as shown in Appendix A.

If we define the symmetric and antisymmetric parts of the eigenfunctions  $\Phi$  as

$$\Phi_k^+(\theta) = \Phi_k(\theta) + \Phi_{-k}(\theta) \quad (21)$$

and

$$\Phi_k^-(\theta) = \Phi_k(\theta) - \Phi_{-k}(\theta), \quad (22)$$

and apply Eqs. (19) and (20), Eq. (17) splits up into the following equations

$$\sum_{l=0}^{\infty} \int_0^\pi d\theta_2 (\sin\theta_1 \sin\theta_2)^{1/2} (K_{2m2l} + K_{2m-2l}) \Phi_{2l}^+(\theta_2) = \lambda \Phi_{2m}^+(\theta_1) \quad (23)$$

$$m, l = 0, 1, 2, \dots,$$

$$\sum_{l=0}^{\infty} \int_0^\pi d\theta_2 (\sin\theta_1 \sin\theta_2)^{1/2} (K_{2m2l} - K_{2m-2l}) \Phi_{2l}^-(\theta_2) = \lambda \Phi_{2m}^-(\theta_1) \quad (24)$$

$$m, l = 0, 1, 2, \dots$$

For the odd terms, two analogous equations can be derived. The resulting four subsets form the basis of our computations, which will be discussed in the next section.

### III. NUMERICAL APPROACH

As it is not possible to solve the four equations derived in the previous section analytically, the eigenfunctions and eigenvalues will be approximated by numerical methods. First we discretize the integral equations into matrix equations, following a method described by Blume *et al.*<sup>3</sup> To this end the integrals over  $\theta_2$ , occurring in each subset, are approximated by a summation, using a Gauss integration formula. Proceeding by example, Eq. (23) is replaced by

$$\sum_{i=0}^{\infty} \sum_{j=1}^N w_j (\sin\theta_1 \sin\theta_2^{(j)})^{1/2} \times [K_{2m2l}(\theta_1, \theta_2^{(j)}) + K_{2m-2l}(\theta_1, \theta_2^{(j)})] \times \Phi_{2l}^+(\theta^{(j)}) = \lambda \Phi_{2m}^+(\theta_1) \quad (25)$$

in which  $N$  is the number of integration points, and  $w_j$ ,  $\theta_j^{(i)}$  are the weights and abscissas of the integration method, respectively. Next we define

$$\psi_k^+(\theta^{(i)}) = \sqrt{w_i} \Phi_k^+(\theta^{(i)}) \quad (26)$$

and

$$H_{2m2l}(\theta^{(i)}, \theta^{(j)}) = \sqrt{w_i w_j} (\sin \theta^{(i)} \sin \theta^{(j)})^{1/2} \\ \times [K_{2m2l}(\theta^{(i)}, \theta^{(j)}) \\ + K_{2m-2l}(\theta^{(i)}, \theta^{(j)})] \quad (27)$$

If we choose a set of values for  $\theta_1$  identical to the abscissas used for  $\theta_2$ , the following set of matrix eigenvalue equations is obtained

$$\sum_{l=0}^{\infty} \sum_{i=1}^N H_{2m2l}(\theta^{(j)}, \theta^{(i)}) \psi_{2l}^+(\theta^{(i)}) = \lambda \psi_{2m}^+(\theta^{(j)}), \quad (28)$$

$$i, j = 1, 2, \dots, N, \quad m, l = 0, 1, 2, \dots,$$

where  $H_{2m2l}$  is a real symmetric  $N \times N$  matrix. The subscripts 1 and 2 have been omitted for convenience. To handle these equations numerically, further approximations are necessary, due to the infinite summation over  $l$ , and the infinite number of equations  $m$ . Fortunately, it can be shown that, if the deviations from uniaxial symmetry are small,  $K_{ml}$  is a sharp-peaked function around  $|m-l|=0$ . In the ideal case of uniaxial symmetry,  $K_{ml}$  is a  $\delta$  function, as shown in Appendix A. Therefore, for a given value of  $m$ , only a few terms in the summation over  $l$  have to be retained, which implies that it is sufficient to consider only a few matrices  $H_{2m2l}$ . On the other hand, only a restricted number of equations  $m$  have to be taken into account. In the uniaxial case only  $m=0$  or  $1$  terms contribute to the physically interesting variables like susceptibility, correlation length, etc.<sup>3</sup> It can be shown that, as long as the deviations from uniaxial symmetry are small, the major contribution is still given by the matrix elements with low values of  $m$ .

We will exploit these features in the following way. Because of the rapid decrease of importance of the matrix elements belonging to increasing values of  $|m-l|$ , we will neglect all submatrices with  $|m-l| > 2k$ ,  $k$  denoting the order of the approximation involved. Furthermore, only  $k$  equations will be retained, because of the second argument given above. In this way Eq. (28) reduces, e.g., for  $k=2$ , to

$$\begin{pmatrix} H_{00} & H_{20} \\ H_{02} & H_{22} \end{pmatrix} \begin{pmatrix} \psi_0^+ \\ \psi_2^+ \end{pmatrix} = \lambda \begin{pmatrix} \psi_0^+ \\ \psi_2^+ \end{pmatrix} \quad (29)$$

It is obvious that, for a given value of  $k$ , the original problem of solving the eigenfunctions and eigenvalues for four infinite sets of coupled integral equa-

tions has been reduced to the solution of four  $N \times k$  matrix eigenvalue equations. These equations can be handled with standard computer routines. In some cases the actual calculation of physical variables may be simplified by general symmetry arguments which lead to a further reduction of the number of equations to be calculated. For details on this subject we refer to Appendix B.

It will be clear from the arguments given above that there are two inherent limitations to the present computational method. First, higher-order approximations, involving the solution of larger matrices, will be needed if the deviations from uniaxial symmetry increase. It appears that the effective magnitude of these deviations can be characterized by the value of  $e_{xy}/T^*$ , where

$$T^* = kT/2|J|S(S+1)$$

Secondly, at low temperatures, the number of integration points  $N$  needs to be increased due to a less smooth behavior of the kernel. Both these effects imply that the temperature ultimately sets a limit to the applicability of the computational method.

In general, the accuracy of the computations was checked by using increasing values of  $N$  and  $k$  until a good convergence was obtained. On the other hand, the results were compared with all known limiting cases, and were found to be identical. A good convergence was generally obtained for  $N \times k = 96$ , at least for  $T^* > 0.03$ . To retain sufficient accuracy at lower temperatures it appeared to be necessary to increase  $N \times k$  roughly proportional to  $T^{-3}$ . Therefore, only a slight decrease of the lower temperature bound already involves an enormous increase in computer time. In the next section we will confine ourselves to the results obtained for  $T^* \geq 0.03$ .

#### IV. RESULTS AND DISCUSSION

With the theory outline above, it is possible to calculate a number of thermodynamic properties of classical chains with orthorhombic anisotropy with or without a field. These properties include the zero-field susceptibility ( $\chi$ ) in several directions, the staggered susceptibility ( $\chi_{st}$ ), and the correlation length ( $\xi$ ). Some of the results have been reported in earlier publications.<sup>6,7,21</sup> In this section we would particularly like to emphasize and illustrate the influence of anisotropy in terms of crossover from one model system to another as a function of temperature or field, as well as the behavior of the ordering temperature of quasi-one-dimensional systems as a function of various parameters, such as the anisotropy, or the interchain interaction  $J'/k$ .

To start with, we return to the model systems introduced in Table I which, in a sense, can be seen as limiting cases in terms of anisotropy. To illustrate

the largely different behavior of these "model systems" and thus the importance of a consistent nomenclature we calculated the inverse correlation length  $\kappa$  as a function of temperature, within the classical spin formalism. The expression relating  $\kappa$  to the computed eigenvalues and eigenvectors is given in Appendix B. The results are shown in Fig. 2. For the cases with a spin dimensionality  $n=3$ , i.e., Heisenberg,  $XY$ , and  $Z$ , the results were obtained from computations with the model described in the previous sections. For  $n=2$  we proceeded in a similar way.<sup>8</sup> The curve shown for  $n=1$  is the exact expression for the inverse correlation length in an  $S = \frac{1}{2}$  quantum mechanical Ising system.<sup>18</sup> This latter system is, in fact, identical to the ( $n=1$ ) classical case (two discrete orientations or states per site).

As argued above a clear distinction must be made between, for instance, the ( $n=3$ )  $XY$  model and the ( $n=2$ ) planar model, and between the ( $n=3$ )  $Z$  model and the ( $n=1$ ) Ising model. Let us first consider the difference between the  $XY$  model and the planar model. In the former model, which is represented by the Hamiltonian Eq. (9) with  $e_z = -1$ ,  $e_{xy} = 0$ , the interaction between the spins has only components in the  $XY$  plane, but the spins themselves are free to have a component in the  $z$  direction. In the planar model, however, the spins are

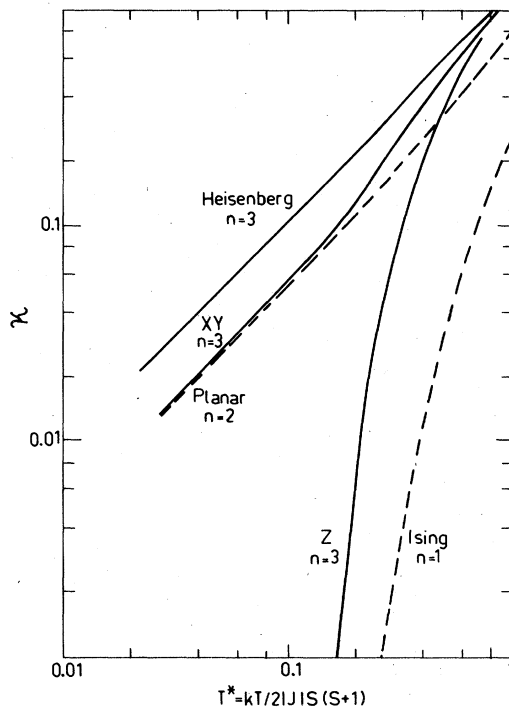


FIG. 2. Inverse correlation length of the spin components along the preferred direction for different 1D model systems vs reduced temperature  $T^*$ .

confined to the  $XY$  plane. It is obvious from Fig. 2 that the  $XY$  model will approach the planar model at low values of the reduced temperature

$$T^* = kT/2|J|S(S+1) \ll 1.$$

For high temperatures ( $T^* \geq 1$ ) the system behaves like an isotropic Heisenberg model. This can be explained by the thermal motion of the spins, which introduces a nonzero expectation value of the spin components in the  $z$  direction at higher reduced temperatures, even though  $J_{zz} = 0$ . In a similar way the  $Z$  model can be distinguished from the Ising model. The  $Z$  model, in which the interaction parameter  $J$  has only a component in the  $z$  direction, is represented by the Hamiltonian Eq. (9) with  $e_z = 2$ ,  $e_{xy} = 0$ . Again the spins can rotate freely, giving rise to an isotropic behavior at high temperatures. This is in marked contrast to the ( $n=1$ ) Ising system.

The observed crossover from one model system to another is also illustrated by the behavior of  $\langle s_\alpha^2 \rangle$  as a function of  $T^*$  for the three components  $\alpha = x, y, z$ , plotted in Fig. 3. Results are presented for two different values of the anisotropy parameter  $e_{xy}$ . The value of  $e_z$  is chosen negative, in which case the spins favor an orientation within the  $XY$  plane. The values of  $e_{xy}$  are chosen as small positive numbers, which implies that the spins tend to be directed toward the  $x$  axis. Inspection of the figure shows that in the high-temperature region the system behaves like an isotropic Heisenberg system ( $n=3$ ), for which all expectation values equal  $\frac{1}{3}$ . This fact is in agreement with the behavior of the correlation length discussed above. At lower temperatures the effect of  $e_z$  becomes noticeable and the system behaves as a ( $n=2$ ) planar system, i.e.,  $\langle s_x^2 \rangle = \langle s_y^2 \rangle = \frac{1}{2}$ ,  $\langle s_z^2 \rangle = 0$ . For still lower temperatures, also the influence of  $e_{xy}$  becomes important and a crossover to an

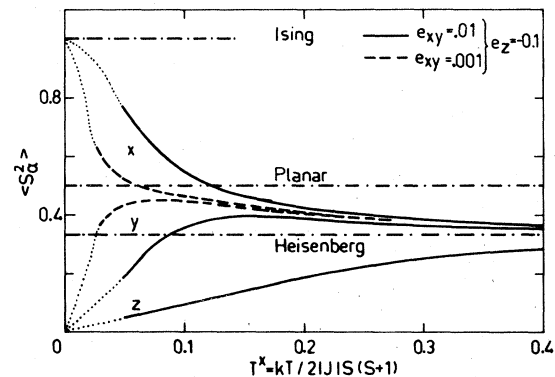


FIG. 3. Expectation value of the spin components  $\langle s_\alpha^2 \rangle$ ,  $\alpha = x, y, z$ , as a function of reduced temperature. The dashed-dotted lines represent the limiting cases. Note that both curves for  $\langle s_z^2 \rangle$  coincide.

Ising-like behavior occurs ( $\langle s_x^2 \rangle = 1$ ). From these observations it can be concluded that in real systems a crossover to Ising behavior can be expected at low temperatures, provided that orthorhombic terms are not forbidden by symmetry. On the other hand, it can be shown that in antiferromagnetic systems with only uniaxial anisotropy a crossover to Ising-like behavior can be induced by an external magnetic field. To illustrate this effect, the inverse correlation length is plotted in Fig. 4 as a function of  $T^*$  for two values of  $H^* = g\mu_B H/2|J|\tilde{S}$ . The system shown in the figure has a small negative value of  $e_z$ , which will cause planarlike behavior at low temperatures. When an external magnetic field is applied parallel to the  $XY$  plane, the system shows a crossover to an Ising-like system, similar to the crossover that would have been induced by anisotropy in the same plane. The reduction of the effective spin dimensionality by an external magnetic field has been predicted by Villain and Loveluck,<sup>22</sup> who argued that this reduction may be the reason for the observed anomalous increase of the Néel temperature in *quasi-one-dimensional* systems, when a field is applied. This point has been

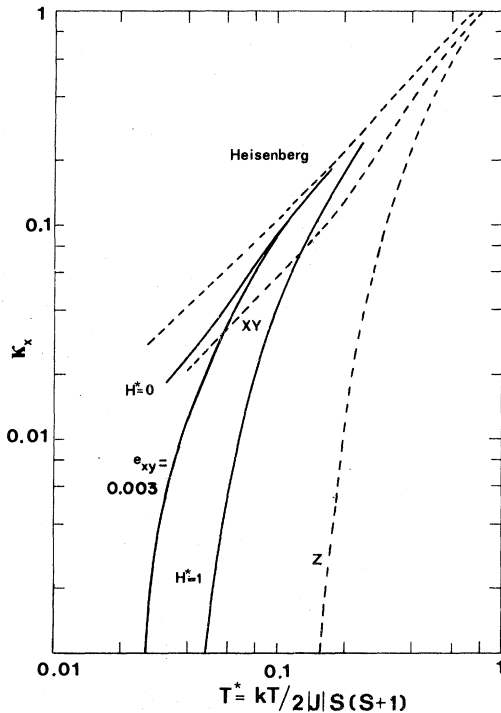


FIG. 4. Inverse correlation length vs reduced temperature for a chain with a small easy-plane anisotropy,  $e_z = -0.01$ , displaying a crossover from Heisenberg to  $XY$ . The other drawn curves show the effect of either a magnetic field applied parallel to the easy plane ( $\vec{H}^* \parallel y$ ), or a small anisotropy in that plane ( $e_{xy} = 0.003$ ). Both curves demonstrate  $XY$ - $Z$  crossover. Dashed lines denote the zero-field limiting cases.

discussed in earlier publications.<sup>6</sup> In principle, in an isotropic ferromagnetic system, a crossover to Ising could also be induced by an external magnetic field. Since, however, the field induced crossover in systems with antiferromagnetic coupling is far more interesting, both experimentally and theoretically, the remainder of this paper will be devoted to the latter case.

Let us now consider the behavior of the inverse correlation length as a function of the external magnetic field somewhat more in detail, especially for low values of  $H$ . In one of the many papers devoted to the behavior of  $(CD_3)_4NMnCl_3$  (TMMC) in a magnetic field, Borsa<sup>9</sup> argued that the correlation length in an isotropic Heisenberg system would increase quadratically with  $H/T$ . His arguments were based on perturbation theory. A similar behavior was predicted for the pure planar case. In order to confront these predictions with our computations, the reduced inverse correlation length  $\kappa/\kappa_0$  is plotted in Fig. 5 as a function of  $H^*/T^*$ . The drawn curves represent the results obtained from numerical calculations on the isotropic model. The upper curve was computed for  $T^* = 0.1$ , while the lower was obtained for  $T^* = 0.05$ . The dashed curves represent the results of the perturbation theory. Due to the fact that this theory is based on a decimation procedure, which is essentially a low-temperature approximation, it predicts a slightly incorrect value of  $\kappa_0$ . Therefore the correlation length is presented in reduced form. For low values of the magnetic field the perturbation

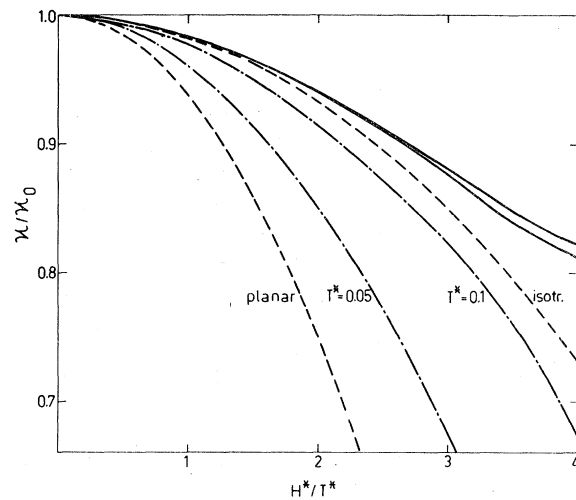


FIG. 5. Reduced inverse correlation length of a classical chain vs  $H^*/T^*$ . Dashed curves are obtained from perturbation theory (Ref. 9) for the isotropic and planar case. Drawn curves represent computations on an isotropic model at two different values of the reduced temperature ( $T^* = 0.05, 0.1$ ). Dashed-dotted curves denote an anisotropic case, with  $e_z = -0.01$ , at the same reduced temperatures.

theory yields correct results. Moreover, in this region, the correlation length depends only on the scaling variable  $H^*/T^*$ . For higher values of the magnetic field, however, this variable is no longer a correct scaling variable, which is illustrated by the splitting of the two drawn curves. Furthermore,  $H^*/T^*$  cannot be used as a scaling variable anymore when an anisotropy is introduced. This is demonstrated by the two dashed-dotted curves, representing an arbitrarily chosen anisotropic case for two temperatures. If the decrease of the correlation length is written as<sup>9</sup>

$$\frac{\kappa}{\kappa_0} = 1 - \frac{1}{C} \frac{H^{*2}}{T^{*2}}, \quad (30)$$

the value of  $C$  amounts to 60 for the isotropic Heisenberg case, and to 16 for the pure planar case. For the anisotropic cases in between, the coefficient  $C$  gradually decreases as a function of the anisotropy and increases as a function of temperature, demonstrating again the competition between  $e_z$  and  $T^*$ .

It would be interesting to compare computations on the correlation length directly with relevant experimental data. Unfortunately, however, measurements on the correlation length are difficult to perform and the reported evidence is rather scarce. Only recently some results were obtained on TMMC by Boucher *et al.*<sup>23</sup> Given the very low reduced ordering temperature of TMMC, the correlation length of a highly isolated chain could be studied down to rather low values of  $T^*$ . The results could be fairly well described by the planar model, as demonstrated by Loveluck.<sup>17</sup> In terms of the results discussed above, the fact that this model correctly explains the observed behavior of TMMC originates from the pronounced easy-plane anisotropy in this compound, giving rise to a crossover from Heisenberg to planar already at values of  $T^*$  higher than the experimental region. In systems, however, where both anisotropy and magnetic field have a comparable effect, or at higher values of the reduced temperature, the behavior of physical variables would be better predicted by the ( $n=3$ ) model, described in this paper. Unfortunately, no experimental data on  $\xi$  are available for other compounds.

We will now direct our attention to the three-dimensional ordering temperature of *quasi*-one-dimensional systems, i.e., systems in which the isolated chains are coupled by small interchain interactions  $J'/k \ll J/k$ . It has been argued<sup>22</sup> that three-dimensional ordering in such systems is largely induced by the correlation length within the individual chains. This mechanism may be represented by the expression

$$|J'|S^2\xi(T_N) = C_n k T_N, \quad (31)$$

where  $J'$  is the interaction between the chains, and  $C_n$  is a constant depending on the spin dimensionality

$n$ . Instead of this rather intuitive relation, a somewhat more consistent formula can be derived by treating the interchain interactions  $J'/k$  in a mean-field approach. This leads to the expression<sup>24</sup>

$$2zJ'\chi_{st}(T_N) = 1, \quad (32)$$

where  $\chi_{st}$  is the staggered susceptibility of an individual—antiferromagnetic—chain, and  $z$  is the number of nearest-neighbor chains.

In principle, Eq. (32) offers the opportunity to study the effect of several variables on the ordering temperature of quasi-one-dimensional systems, which is straightforward in the case of  $J'/k$ . However, several other variables have an effect on the ordering temperature, through their effect on  $\chi_{st}$ . These variables include the anisotropy, an external magnetic field, and, for instance, the concentration of diamagnetic impurities. The effect of the latter two variables has already received extensive attention in the literature,<sup>7,25</sup> and will therefore only be reviewed very shortly at the end of this section. Now, we will first consider the effect of  $J'/k$ , since this allows us to investigate the validity of the mean-field approximation of the interchain interactions and hence Eq. (32), by comparing the predicted behavior with exactly solvable models.

In Fig. 6 the reduced ordering temperature  $T_N^*$  for different model systems is plotted. The limiting cases Heisenberg and Z are computed from the classical model. Furthermore an arbitrary anisotropic system is shown. For comparison, the prediction for an Ising system<sup>26</sup> and a prediction following from Green's-function theory for a Heisenberg system<sup>27</sup> are included in the figure. Also a calculation is presented in

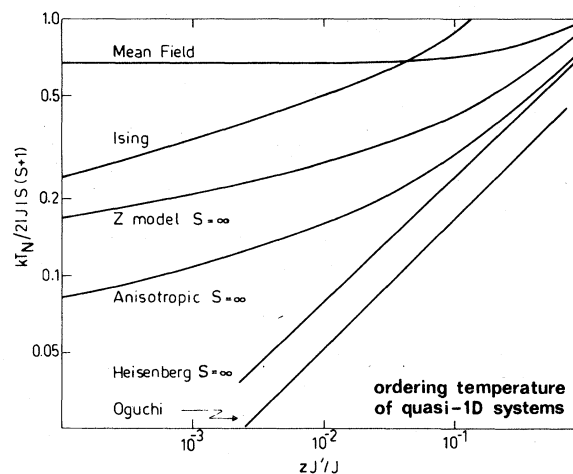


FIG. 6. Predicted behavior of the reduced ordering temperature of quasi-one-dimensional systems as a function of the interchain interaction  $zJ'/J$  for various model systems within several approximations.



which both  $J$  and  $J'$  are treated within the mean-field approximation. Assuming the Green's-function theory to give the most reliable value of the ordering temperature, it is clear that if all interactions are treated within the mean-field approximation, the predicted value of  $T_N^*$  for quasi-one-dimensional systems is much too high. Moreover, the predicted value is almost independent of the value of  $J'$ . This is not surprising, given the fact that the mean-field theory yields a finite ordering temperature, even in the purely one-dimensional case. The classical Heisenberg case, according to Eq. (32), in which only  $J'$  is treated within the mean-field approximation, shows a behavior very much alike the Oguchi case. The only difference is a small shift towards higher ordering temperatures, which most probably reflects mean-field effects in Eq. (32). The qualitative dependence of  $T_N^*$  on the parameter  $zJ'/J$  is predicted correctly. Hence, if we apply the results from the classical model to determine only relative changes of the ordering temperature, errors induced by the observed shift are eliminated. Moreover, the results strongly suggest that Eq. (32) is a very good approximation of the actual relation between  $\chi_{st}$  and  $T_N$  for quasi-one-dimensional systems.

Further inspection of Fig. 6 shows that the effect of anisotropy is most pronounced for low values of  $zJ'/J$ . At higher values of  $zJ'/J$ , the ordering temperatures for different values of the anisotropy, at least for systems with the same spin dimensionality  $n$ , all converge to the same value. Unfortunately, there is no direct experimental evidence on the magnitude of  $J'$ , except for some quasi-one-dimensional Ising systems, where the interchain coupling can be determined by spin cluster resonance techniques.<sup>28</sup>

In view of the drastic effect of even a small amount of anisotropy, we will next consider the ordering temperature as a function of the anisotropy. We characterize the anisotropy by the parameters  $\alpha$  and  $\beta$ .  $\alpha$  denotes the reduced energy difference between two antiferromagnetically ordered states of the system, aligned along the easy axis and the intermediate axis, respectively. The reduced energy gap between the easy and hard axis will be denoted by  $\beta$

$$\alpha = \frac{\Delta E_{ie}}{2|J|S(S+1)}, \quad \beta = \frac{\Delta E_{he}}{2|J|S(S+1)} \equiv \alpha x, \quad (33)$$

$$x \geq 1.$$

For  $x < 1$ , the intermediate and hard axes interchange.

The behavior of the ordering temperature as a function of the parameter  $\alpha$  is plotted in Fig. 7 for different values of  $x$ . The curves were obtained by calculating the reduced ordering temperature, according to Eq. (32), for a given value of  $zJ'$ . The figure shows the cases  $x=0$ , corresponding to an easy-plane type of anisotropy, and  $x=1$ , in which case the inter-

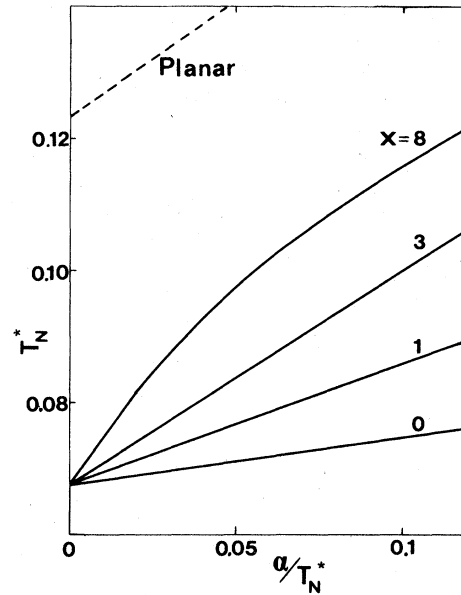


FIG. 7. Reduced ordering temperature of a system of loosely coupled antiferromagnetic chains as a function of the anisotropy for a constant value of  $zJ'/J (= 7 \times 10^{-3})$ . The meanings of  $\alpha$  and  $x$  are explained in the text.

mediate and hard axes are identical. Furthermore, two curves are shown for higher values of  $x$ . For comparison, results obtained from the planar model, using Eq. (32) and the same value of  $zJ'$  are plotted also. For small values of the anisotropy gaps,  $T_N^*$  appears to be a linear function of  $\alpha/T_N^*$ , suggesting

$$T_N^* = C_1 + C_2 \alpha / T_N^*. \quad (34)$$

This formula is quite analogous to a relation between the ordering temperature and the single-ion anisotropy  $D$ , derived for instance by Shapira.<sup>29</sup> In these derivations all interactions were treated in the mean-field approximation. The linear behavior of  $T_N^*$  with  $\alpha/T_N^*$  disappears for higher values of the energy gaps, which is most clearly demonstrated by the curve for  $x=8$ . The constants  $C_1$  and  $C_2$  depend on the value of  $zJ'$ .

Finally, we would like to make some concluding remarks. The anomalous field dependence of the ordering temperature, observed in many quasi-one-dimensional systems built up from antiferromagnetic chains, could be explained fairly well by the present model, at least for systems with  $S = \frac{5}{2}$ . For details we refer to earlier publications on this subject.<sup>6,7</sup> On the other hand, it is possible to include the effect of diamagnetic impurities with only slight modifications of the theory presented above.<sup>25</sup> The resulting model was found to give a good description of the experimentally observed decrease of  $T_N^*$  with impurity concentration in a number of quasi-one-dimensional

manganese compounds. Also the field dependence of  $T_N^*$  in the presence of diamagnetic impurities could be described satisfactorily.

In summary, we would like to state that all experimental evidence available at this moment indicates that, for  $S \geq \frac{5}{2}$ , the present theory satisfactorily describes the behavior of an isolated chain as well as the three-dimensional ordering temperature of quasi-one-dimensional systems, provided that the anisotropy is properly taken into account.

#### ACKNOWLEDGMENTS

The authors wish to acknowledge the significant contribution of Dr. J. P. A. M. Hijmans, especially in

the early stage of this work. We would also like to thank A. M. C. Tinus for his assistance in the numerical computations. This work is partially supported by the Stichting Fundamenteel Onderzoek der Materie.

#### APPENDIX A

In this appendix we will consider, without loss of generality, the case in which the anisotropy entirely originates from anisotropic terms in the exchange interaction, i.e.,  $H_{si} = 0$ . In that case, substitution of Eq. (12) into Eq. (18), making use of Eqs. (4), (9), and (10), yields the following expression for the kernel

$$K_{ml}(\theta_1, \theta_2) = \Theta(\theta_1, \theta_2) \frac{1}{2\pi} \int_{-\pi}^{\pi} d\phi_1 \int_{-\pi}^{\pi} d\phi_2 \exp\{A(\theta_1, \theta_2) [(1 - \frac{1}{2}e_z) \cos(\phi_1 - \phi_2) + \frac{1}{2}e_{xy} \cos(\phi_1 + \phi_2)]\} e^{-im\phi_1} e^{il\phi_2}, \quad (A1)$$

where

$$\Theta(\theta_1, \theta_2) = \exp[\beta 2J\bar{S}^2(1 + e_z) \cos\theta_1 \cos\theta_2 + \frac{1}{2}\beta g\mu_B H\bar{S}(\cos\theta_1 + \cos\theta_2)] \quad (A2)$$

is the purely  $\theta$ -dependent part of the integral, and

$$A(\theta_1, \theta_2) = \beta 2J\bar{S}^2 \sin\theta_1 \sin\theta_2. \quad (A3)$$

By substituting

$$m = n + k, \quad l = n - k, \quad (A4)$$

and introducing the new variables,

$$x = \phi_1 + \phi_2, \quad y = \phi_1 - \phi_2, \quad (A5)$$

$K_{ml}$  can be written as

$$K_{ml}(\theta_1, \theta_2) = \Theta(\theta_1, \theta_2) \frac{1}{2\pi} \int_{-\pi}^{\pi} dx \exp[\frac{1}{2}e_{xy}A(\theta_1, \theta_2) \cos x] e^{-ikx} \int_{-\pi}^{\pi} dy \exp[(1 - \frac{1}{2}e_z)A(\theta_1, \theta_2) \cos y] e^{-iny}, \quad (A6)$$

where the  $2\pi$  periodicity of the functions involved has been used. With the aid of the well-known integral formulas<sup>30</sup>

$$\int_{-\pi}^{\pi} d\phi \exp(p \cos\phi) \sin(m\phi) = 0, \quad (A7)$$

and

$$\int_{-\pi}^{\pi} d\phi \exp(p \cos\phi) \cos(m\phi) = 2\pi I_m(p), \quad (A8)$$

where  $I_m(p)$  is the modified Bessel function of order  $m$ , Eq. (A6) can be written as

$$K_{ml}(\theta_1, \theta_2) = \Theta(\theta_1, \theta_2) 2\pi I_{(m-l)/2}(\frac{1}{2}e_{xy}A(\theta_1, \theta_2)) \times I_{(m+l)/2}(A(\theta_1, \theta_2)(1 - \frac{1}{2}e_z)) \quad (A9)$$

If uniaxial symmetry is present, i.e.,  $e_{xy} = 0$ , Eq. (A9)

reduces to

$$K_{ml}(\theta_1, \theta_2) = 2\pi I_m(A(\theta_1, \theta_2)(1 - \frac{1}{2}e_z)) \times \Theta(\theta_1, \theta_2) \quad (A10)$$

Only the terms with  $m = l$  are nonzero, because of the property of the modified Bessel function

$$I_k(0) = \delta_k, \quad (A11)$$

where  $\delta$  is the Kronecker  $\delta$ . The special case, given by Eq. (A10) is in agreement with results reported in the literature.<sup>3</sup>

#### APPENDIX B

In this appendix the formulas which we used to describe the thermodynamic properties of the classi-

cal chain will be presented. These properties will be expressed in the eigenfunctions and eigenvalues of the four Eqs. (23), (24), etc. It can be easily deduced that the two-spin correlation function  $\langle s_j^\alpha s_{j+q}^\beta \rangle$ , where  $\alpha, \beta = x, y, z$ , can be expressed as

$$\langle s_j^\alpha s_{j+q}^\beta \rangle = \sum_{i=1}^4 \sum_{n=0}^{\infty} \left( \frac{\lambda_{in}}{\lambda_{10}} \right)^q \int d\bar{s}_j \psi_{\Gamma_{i,n}}(\bar{s}_j) s_j^\alpha \psi_{\Gamma_{1,0}}(\bar{s}_j) \int d\bar{s}_{j+q} \psi_{\Gamma_{1,0}}(\bar{s}_{j+q}) s_{j+q}^\beta \psi_{\Gamma_{i,n}}(\bar{s}_{j+q}), \quad (\text{B1})$$

where  $\lambda_{in}$  is the eigenvalue belonging to the eigenfunction  $\psi_{\Gamma_{i,n}}$ , which transforms according to the  $i$ th irreducible representation  $\Gamma_i$  of the group  $C_{2v}$ . It can be shown, that only a restricted number of integrals in Eq. (B1) will contribute to the correlation functions, due to the symmetry of the group. The remaining terms can be written as

$$\langle s_j^\alpha s_{j+q}^\beta \rangle = \delta_{\alpha,\beta} \sum_{n=0}^{\infty} \left( \frac{\lambda_{in}}{\lambda_{10}} \right)^q \left| \int d\bar{s} \psi_{\Gamma_{i,n}}(\bar{s}) s^\alpha \psi_{\Gamma_{1,0}}(\bar{s}) \right|^2, \quad (\text{B2})$$

where  $i=1$  for  $\alpha=z$ ,  $i=3$  for  $\alpha=x$ , and  $i=4$  for  $\alpha=y$ ,<sup>31</sup> and  $\delta_{\alpha,\beta}$  is the Kronecker  $\delta$ .

The wave-vector-dependent susceptibility is deduced from these correlation functions with the fluctuation-dissipation relation<sup>4</sup>

$$\chi^\pi(k) = \beta \left[ \langle s_0^\pi s_0^\pi \rangle - \langle s_0^\pi \rangle^2 + 2 \sum_{q=1}^{\infty} \cos(qk) (\langle s_0^\pi s_q^\pi \rangle - \langle s_0^\pi \rangle^2) \right]. \quad (\text{B3})$$

For  $k=0$  and  $\pi$  the normal and the staggered susceptibility are obtained, respectively. The inverse correlation length can be calculated from the correlation functions, using the definition<sup>5</sup>

$$\kappa_\alpha^2(k) = \frac{1}{\beta} \chi^\pi(k) \left[ \sum_{q=0}^{\infty} q^2 \cos(qk) (\langle s_0^\pi s_q^\pi \rangle - \langle s_0^\pi \rangle^2) \right]^{-1}, \quad (\text{B4})$$

with  $k=0$  for ferromagnetic, and  $k=\pi$  for antiferromagnetic interaction.  $\kappa$  can now be calculated with the aid of Eq. (B2). Proceeding by example, the inverse correlation length for an antiferromagnetic array is given by

$$\kappa_\alpha^2 = \frac{1}{\beta} \chi^\alpha(\pi) \left[ \sum_q (-1)^q q^2 \sum_n \left( \frac{\lambda_{in}}{\lambda_{10}} \right)^q c_n^2 \right]^{-1}, \quad (\text{B5})$$

where

$$c_n^2 = \left| \int d\bar{s} \psi_{\Gamma_{i,n}}(\bar{s}) s^\alpha \psi_{\Gamma_{1,0}}(\bar{s}) \right|^2. \quad (\text{B6})$$

Interchanging the summations over  $n$  and  $q$ , and summing the simple geometric series over  $q$ , leads to

$$\kappa_\alpha^2 = \frac{1}{\beta} \chi_\alpha(\pi) \sum_{n=1}^{\infty} c_n^2 \frac{\lambda_{in}}{\lambda_{10}} \left[ 1 - \frac{\lambda_{in}}{\lambda_{10}} \right] \left[ 1 + \frac{\lambda_{in}}{\lambda_{10}} \right]^3. \quad (\text{B7})$$

In an analogous way other physical properties can be expressed in eigenvalues and eigenfunctions of Eqs. (23), (24), etc.

<sup>1</sup>M. E. Fisher, Am. J. Phys. **32**, 343 (1964); T. Nakamura, J. Phys. Soc. Jpn. **7**, 264 (1952).

<sup>2</sup>See, for instance, M. Steiner, J. Villain, and C. Windsor, Adv. Phys. **25**, 87 (1976).

<sup>3</sup>M. Blume, P. Heller, and N. A. Lurie, Phys. Rev. B **11**, 4483 (1975).

<sup>4</sup>S. W. Lovesey and J. M. Loveluck, J. Phys. C **9**, 3639 (1976).

<sup>5</sup>J. M. Loveluck, S. W. Lovesey, and S. Aubry, J. Phys. C **8**, 3841 (1975).

<sup>6</sup>W. J. M. de Jonge, F. Boersma, and K. Kopinga, J. Magn. Mater. **15-18**, 1007 (1980).

<sup>7</sup>J. P. A. M. Hijmans, K. Kopinga, F. Boersma, and W. J. M. de Jonge, Phys. Rev. Lett. **40**, 1108 (1978).

<sup>8</sup>K. Takeda, T. Koike, T. Tonegawa, and I. Harada, J. Phys. Soc. Jpn. **48**, 1115 (1980).

<sup>9</sup>F. Borsa, J. P. Boucher, and J. Villain, J. Appl. Phys. **49**, 1327 (1978).

<sup>10</sup>H. E. Stanley, Phys. Rev. **179**, 570 (1969).

<sup>11</sup>J. C. Bonner and M. E. Fisher, Phys. Rev. **135**, 640 (1964).

<sup>12</sup>T. de Neef, Phys. Rev. B **13**, 4141 (1976).

<sup>13</sup>S. Katsura, Phys. Rev. **127**, 1508 (1962).

<sup>14</sup>C. J. Thompson, J. Math. Phys. **9**, 241 (1968).

<sup>15</sup>M. Suzuki, B. Tsujiyama, and S. Katsura, J. Math. Phys. **8**, 124 (1967).

<sup>16</sup>C. S. Joyce, Phys. Rev. Lett. **19**, 581 (1967).

<sup>17</sup>J. M. Loveluck, J. Phys. C **12**, 4251 (1979).

<sup>18</sup>E. Ising, Z. Phys. **31**, 253 (1925).

<sup>19</sup>G. S. Joyce, Phys. Rev. **155**, 578 (1967).

<sup>20</sup>R. Courant and D. Hilbert, *Methods of Mathematical Physics* (Interscience, New York, 1953).

<sup>21</sup>W. J. M. de Jonge, J. P. A. M. Hijmans, F. Boersma, J. C. Schouten, and K. Kopinga, Phys. Rev. B **17**, 2922 (1978).

<sup>22</sup>J. Villain and J. M. Loveluck, J. Phys. (Paris) Lett. **38**, L77 (1977).

- <sup>23</sup>J. P. Boucher, L. P. Regnault, J. Rossat-Mignod, J. Villain, and J. P. Renard, *Solid State Commun.* 31, 311 (1979).
- <sup>24</sup>See, for instance, D. J. Scalapino, Y. Imry, and P. Pincus, *Phys. Rev. B* 11, 2042 (1975).
- <sup>25</sup>J. C. Schouten, F. Boersma, K. Kopinga, and W. J. M. de Jonge, *Phys. Rev. B* 21, 4089 (1980).
- <sup>26</sup>See, for example, D. Hone, P. A. Montano, T. Tonegawa, and Y. Imry, *Phys. Rev. B* 12, 5141 (1975), and references therein.
- <sup>27</sup>T. Oguchi, *Phys. Rev.* 133, 1098 (1964).
- <sup>28</sup>Q. A. G. van Vlimmeren and W. J. M. de Jonge, *Phys. Rev. B* 19, 1503 (1979).
- <sup>29</sup>Y. Shapira, *Phys. Rev. B* 2, 2725 (1970).
- <sup>30</sup>I. S. Gradshteyn and I. M. Ryzhik, *Tables of Integrals, Series and Products* (Academic, New York and London, 1965).
- <sup>31</sup>See, for example, M. Tinkham, *Group Theory and Quantum Mechanics* (McGraw-Hill, New York, 1964).